Research Square

Preprints are preliminary reports that have not undergone peer review.
They should not be considered conclusive, used to inform clinical practice,
or referenced by the media as validated information.

A green plasmonic nanosensor based on AuNPs for bacteria detection in urine

A. Ángeles-Pascual (aangelesp@cinvestav.mx)
Center for Research and Advanced Studies of the National Polytechnic Institute
L. Breton-Deval
Universidad Nacional Autónoma de México

Research Article

Keywords: Au nanoparticles, plasmonic nanosensor, green chemistry, urine analysis

Posted Date: June 16th, 2022

DOI: https://doi.org/10.21203/rs.3.rs-1693666/v1

License: This work is licensed under a Creative Commons Attribution 4.0 International License.
Read Full License

Abstract

Today the health problems related to infection by bacteria and virus have increased notably worldwide; for this reason, the demand for reliable and rapid detection methods are necessary. In this work we present a study of colorimetric bacteria in the urine based on 4-mercaptophenylboronic acid (4-MPBA) functionalized with gold nanoparticles (AuNPs) as a green plasmonic nanosensor (GPN) synthesized via novel and simple hand-made *Cinnamomum verum* extract by green chemistry. Three molar concentrations of AuNPs were synthesized (1, 2 and 3 mM). The structural characterization results by X-ray diffraction (XRD) indicated the presence of AuNPs, chemical and morphological analysis by high-resolution field emission scanning electron microscopy (HR-FESEM) technique indicated the presence of AuNPs and size distribution of 15, 37 and 135.5 nm, respectability, being 1 mM the concentration the one that produces AuNPs with size control and good dispersion and used to determine the bacterial quantification at concentrations of N1 = 60 mg, N2 = 105 mg and N3 = 120 mg of AuNPs. The urine concentrations were analyzed in the absorbed light in the UV region at different bacteria concentrations, been the concentrations of 120 mg that showed best linear relationship between the absorbance at 534 nm and was the ideal to achieve an equilibrium between the free bacteria and the nanoparticles.

Background

Urinary tract infections (UTIs) affect around 150 million people worldwide. UTIs are caused by *Escherichia coli* and other pathogens such as *Klebsiella pneumoniae*, *Staphylococcus saprophyticus*, *Enterococcus faecalis*, *Proteus mirabilis*, *Pseudomonas aeruginosa*, and *Staphylococus aureus* [1]. The diagnostic of UTIs is the traditional urine culture with their respective antibiogram. However, this process takes around two days. In contrast, other techniques such as Polymerase Chain Reaction (PCR), flow cytometry, and Enzyme-Linked Immunosorbent Assay (ELISA) are rapid but costly [2]. Because of this, clinical usually initiate empirical antibiotic treatments without laboratory evidence increasing the number of antibiotic-resistant pathogens. At present, more than half of patients in Japan present resistance to fluoroquinolone antibiotics in *Escherichia coli* (E. *coli*) used for UTIs treatment [3]. Another problem in the UTIs diagnostic is the number of samples that arrive to be processed every day. Laboratories used various analyses to decide which urine samples should be cultured. However, this is time-consuming and imprecise [4]. Recently, the use of AuNPs in the development of diagnostic methods has shown promising results, providing low-cost and quicker diagnostics. Gold nanoparticles (AuNPs) have been studied as colloidal systems since 1857 by Michael Faraday [5] and due to their biocompatibility and properties, they are currently an exceptional candidate in biomedical diagnosis [6]. AuNPs have plasmon resonance properties when light is reflected through tiny metal layers modify the charge-density distributions originated at the metal interface [7]. Various synthesis methods have been applied to obtain gold nanostructured systems with homogeneous shapes and size distribution [8, 9], however, the disadvantage of using chemicals in the synthesis is the toxicity, directly impacting the environment by polluting natural resources [10] and affecting human health from exposure to chemicals inherent to their toxic properties [11]. Due to these disadvantages, the study of alternative synthesis routes to obtain different

nanostructured systems has attracted attention in recent years, called green chemistry [12, 13]. Currently, various studies report using plant extracts such as; algae [14], bacteria and fungi [15] are alternative for the reduction and stabilization of nanoparticles. Two main advantages of green chemistry can be mentioned; first, it is an environmentally friendly method because extracts are used. Second, the cost is relatively lower, making green chemistry an alternative in the synthesis of nanoparticles [16]. Several studies have already been conducted using plant extracts, especially *Cinnamomum verum extract*, which is being extensively studied due to its properties to produce nanoparticles as a prospect uses in medicinal and antibacterial agents [17, 18]. Even recent studies report the synthesis of *Cinnamomum verum* nanoparticles with truncated tetrahedral forms for medical applications [19]. This study aims to demonstrate a simple hand-made easy way to obtain AuNPs with *Cinnamomum verum extract* to study colorimetric bacteria in the urine based on 4-MPBA functionalized with AuNPs as a green plasmonic nanosensor in order to close the gap between the generation of nanoparticles from biological systems and the application in biomedical nanotechnology.

Methods

Cinnamomum verum extract preparation

Cinnamomum verum bark from Orizaba, state of Veracruz, México, was used, 10 g were previously weighed and placed in 500 ml of deionized (DI) water in a one-liter flask at boiling temperature for 10 min. Once the boil is reached, it is allowed to cool down to room temperature, and it is strained with filter paper number one for its later use.

Synthesis of gold nanoparticles

In order to fabricate gold nanoparticles (AuNPs), gold (III) chloride trihydrate ($HAuCl_4 \cdot 3H_2O$) as a precursor with purity ≥ 99.9 % was purchased by Sigma Aldrich and DI water was used throughout the experiment. Then the previously prepared *Cinnamomum verum* extract was used, and the procedure was as follows; Three molar ratio of 1, 2, and 3 mM of $HAuCl_4 \cdot 3H_2O$ were mixed in to 10 ml of DI water respectively; once the solutions were prepared dropwise were added to 6 ml of *Cinnamomum verum* extract, respectively with continuous stirring and these gradually changed from light brown to darker shades and deep wine color, indicating the reduction of Au^+ and the formation of AuNPs in all concentrations.

Mechanism growth of AuNPs in presence of Cinnamomum verum extract

During the generation of Au seeds, *Cinnamomum verum* extract plays an important role, because its main chemical compounds, including cinnamaldehyde, cinnamyl acetate, cinnamic acid and eugenol [20] are responsible of the process for the reduction of Au^+ into AuNPs (Fig. 1).

It has been reported that the cinnamaldehyde chemical compound belongs to group of aldehydes [21] that contains the typical scent and flavor of *Cinnamomum verum* and tend to be easily oxidized, which is

why it is considered a good reducing agent capable of reducing Au^{+} to form small seeds that will grow gradually until forming the first gold nanocrystals. It is also important to mention that not all parts of the plant contain the same chemical compounds, depending on which part of the plant the *Cinnamomum verum* is taken, this will be the amount of the compound present, in general, it has been reported [22] that the bark of *Cinnamomum verum* is composed on average 60 % to 80 % cinnamaldehyde and 5 % to 10 % eugenol, essential compounds as reducing agents.

Functionalization of 4-MPBA on AuNPs

In order to functionalize the AuNPs by a displacement mechanism, 2 mL of 4-MPBA (0.1mM) was added to 3 mL AuNPs solution 1 mM. The nanoparticle solution was previously adjusted to pH = 11 with 0.5 M KOH. The 4-MPBA plus AuNPS solution remain stirring during 12 h at room temperature. At the end, the solution was centrifuged at 8500 rpm for 15 min, the supernatant was decanted and the precipitated was re-dispersed in DI water, this step was repeated five times until the absorption peak of 4-MPBA was not observable.

AuNPs characterization

The fabricated AuNPs was corroborated by X-ray diffraction (XRD) using a Panalytical diffractometer, with Cu-Kα radiation (1.540598 Å) in a range of 2 Theta from 20-100° in steps of 0.0400°. The average crystal size (D) was calculated using the Scherrer's equation ($D = K\lambda/\beta\cos\theta$) [23,24]. The morphology of the AuNPs was analyzed using High-resolution field emission scanning electron microscopy (HR-FESEM) equipment JSM7800F and the chemical analysis (energy dispersive X-Ray spectroscopy, EDS) was performed using an Oxford microanalysis detector coupled to the FESEM. In order to obtain particle size distribution and histograms of AuNPs, Gatan Digital Micrograph® and free software ImageJ [25] were used.

Bacterial culture and detection

A single colony of *E. coli* strain was inoculated in Luria-Bertani medium (LB) to grow (24 h, at 37 °C and shaking at 150 rpm) until the OD600 was 1 x 10^{9} CFU mL. A serial dilution from 10^{8} to 10^{1} CFU/mL were made. Then, bacteria were centrifuged at 5500 rpm for 10 min and suspended in deionized water or urine. The urine sample was selected from a healthy person. The urine has the follow characteristics, (Table 1). However, before being used was filtered with a cellulose membrane of 47 and 22 μm to eliminate any possible bacteria.

Table 1 Chemical characteristics of the urine sample

Parameter	Range
pH	7.2
Specific gravity	1.002 g/ml
Urea	22 g/d
Uric Acid	600 mg/d
Creatinine	964 mg/d
Citrate	864 mg/d
Sodium	150 mmol/d
Potassium	50 mmol/d
Ammonium	35 mmol/d
Calcium	115 mg/d
Magnesium	201 mmol/d
Chloride	189 mmol/d
Oxalate	23 mmol/d
Sulphate	28 mmol/d
Phosphate	26 mmol/d

For bacteria detection, 100 µL *E. coli* at different concentrations were incubated with 100 µL 4-MPBA-AuNPs at three different concentrations, N1 = 60 mg, N2 = 105 mg and N3 =120 mg, in 96 microwell plates for 15 min at 37 °C, then 10 µL NaCl (10 M) was added. The microplate was reading with the UV spectra at 534 nm corresponds to the detection pick. For each sample we performed three independent replicates.

Results And Discussion

AuNPs characterization

The XRD analysis of the AuNPs are shown in the Fig. 2, they exhibit four different diffraction peaks at angles 2 theta, 38.3°, 44.3°, 64.7° and 77.7° corresponding to the standard Bragg reflections (111), (200), (220) and (311) respectability, according to the card JCPDS no.04-0784, an intense peak is observed at 38.3 ° indicating a preferential growth in the (111) direction, other peaks can be observed related to noise during the acquisition process. Subsequently, the average crystal size was calculated according to the

Scherrer's equation, the averages correspond to 10.8, 25.4 and 39.4 nm for concentrations of 1, 2 and 3 mM respectively.

In general, Fig. 3 shows the elemental chemical analysis of the AuNPs synthesized with concentration of 3 mM, the inserted table indicates the presence of gold with 73.70 wt %, the mappings indicate the presence of silicon, chlorine, and oxygen.

In Fig. 4 typical high resolution FESEM images of AuNPs are presented. Figure 4a corresponds to the sample with concentration 1 mM, as the micrographs indicated, the dispersion and size distribution is under control, the inserted histogram (Fig. 4b) indicates an average size of 15 nm ± 3.5 nm. Figure 4c corresponds to the concentration of 2 mM, according to the micrographs it can be clearly seen that the sizes increase, and some morphological icosahedral and decahedral were mainly identified, nevertheless we identified triangular and pentagonal plates, these results suggest if the molar radio increased, the size, shape and dispersion control start to lose gradually, because the particle size distribution histogram increase at an average of 37 nm ± 12 nm (Fig. 4d). Figure 4e correspond to 3 mM concentration, some shapes correspond to icosahedra and decahedrons forms. However more predominant triangular shapes, pentagonal plates, nanobars and nanocubes were observed, according with another groups using *Cinnamomum verum* extract [26]. The histogram of the average particle size distribution (Fig. 4f) corresponds to 135.5 nm ± 92 nm. In general, the changes in the morphology during the growth process suggests that the nucleation and growth was slow and the thermodynamic conditions were suitable for the seeds to grow with different forms as has been suggested by some authors [27]. In general, the predominant morphological forms in the three molar concentrations are nanobars > 100 nm, triangular, pentagonal, hexagonal, truncated nanoplates, icosahedrons and decahedrons also were perfectly identified.

Bacteria Detection And Quantification

The 1 mM AuNPs were selected for the following experiment due to their size, dispersion, and morphology. We select three concentrations of this 1 mM AuNPs to determine the best NPs concentration for bacterial quantification. The concentrations selected where: N1 = 60 mg, N2 = 105 mg and N3 = 120 mg. Figure 5, showed the effect of using different concentrations of functionalized AuNPs to quantify different concentrations of bacteria. Red-line (square symbol) are the responses of functionalized AuNPs at their respective concentration in urine to the absorbed light in the UV region at different bacteria concentrations. The experiments carried out with 60 and 105 mg of AuNPs did not help to evaluate lower concentrations of bacteria 10^1. The blue-line (circle symbol) in all captions showed the response of functionalized AuNPs in water at different bacteria concentrations. As can be seen, the concentrations of the various compounds in urine did not affect the trend of the functionalized AuNPs response. These results are consistent with Huang et al., [28], who evaluated the effect of various ions such as Ca^{2+}, Cu^{2+}, Mg^{2+}, Fe^{3+} Zn^{2+} in the UV-vis response of functionalized AuNPs. Yellow-lines (triangular symbol) in all

captions showed the UV-vis spectroscopy measure without functionalized AuNPs, highlight the necessity to use functionalized AuNPs to quantify small differences in the bacteria concentration.

The experiments with concentrations of 60, 105 and 120 mg of functionalized AuNPs are presented in Fig. 6. The concentrations of 60 and 105 mg showed a linear relationship between the absorbance at 534 nm and *E. coli* concentration (10^1–10^8 CFU/mL). However, at higher concentration of 120 mg of functionalized AuNPs the relationship between the absorbance and the bacteria concentration showed a logarithmic relationship observed in the violet-line (circle symbol) in the graphic. Szunerits et al., [7] observed a change in the relationship between the absorbance and the concentration of analyte trough the time. At the beginning of the experiment the relationship was linear but at advances stages of the experiment, more analyte was added, and all the possible interactions nanoparticle-analyte were filled results in higher refractive index on the nanoparticle. In our case this change in the relationship was due a higher concentration of AuNPs was the ideal to achieve an equilibrium between the free bacteria and the nanoparticles.

Conclusions

A low-cost, rapid and easy study of colorimetric bacteria in urine based on 4-MPBA functionalized with AuNPs as a green plasmonic nanosensor synthetized via simple *hand-made Cinnamomum verum* extract by green chemistry is proposed. The XRD analysis indicate the presence of AuNPs and HR-FESEM indicated significant differences in morphologies as well as icosahedron and decahedral morphologies more predominant. The size distribution for the molar concentration 1, 2 and 3 mM allows to obtain AuNPs with average sizes of 15, 37 and 135.5 nm respectability, being the 1 mM concentration that shows best control of size, dispersion and morphology for the concentration for bacterial quantification. The concentrations of urine selected where: N1 = 60 mg, N2 = 105 mg and N3 = 120 mg been the concentrations of 120 mg that showed best linear relationship between the absorbance via UV region at 534 nm, even do, the concentrations of the various compounds in urine did not affect the trend of the functionalized AuNPs response that make it possible the use in bio detection in urine samples and in the near future in different medical applications as a green plasmonic nanosensor.

Abbreviations

4-MPBA
4-mercaptophenylboronic acid
AuNPs
Gold nanoparticles
GPN
Green plasmonic nanosensor
XRD
X-ray diffraction
HR-FESEM

High-resolution field emission scanning electron microscopy
UV
Ultraviolet
UTIs
Urinary tract infections
PCR
Polymerase chain reaction
ELISA
Enzyme-linked immunosorbent assay
E. coli
Escherichia coli
DI
Deionized
EDS
Energy dispersive spectroscopy
LB
Luria-Bertani.

Declarations

Ethics approval and consent to participate

All authors agreed on the ethics approval and consent to participate.

Consent for publication

Not applicable.

Availability of data and material

Not applicable.

Competing interests

The authors declare that they have no competing interests.

Funding

Not applicable.

Authors' contributions

AA synthesis and characterization of nanoparticles, LB design and performed the bacteria detection in urine, AA-LB carried out the design the project, analysis, discussion and drafted the manuscript, were

involved in experiments. Both authors read and approved the final manuscript and submission.

Acknowledgements

The authors would like to acknowledge to Laboratorio Avanzado de Nanoscopía Electrónica (LANE-Cinvestav) and Laboratorio Central de Microscopía (LCM-IFUNAM).

References

1. Flores-Mireles AL, Walker JN, Caparon M, Hultgren SJ. Urinary tract infections: Epidemiology, mechanisms of infection and treatment options. Nat Rev Microbiol. 2015;13(5):269–84.
2. Sharma A, Agrawal A, Awasthi KK, Awasthi K, Awasthi A. Biosensors for diagnosis of urinary tract infections: Advances and future challenges. Mater Lett X [Internet]. 2021;10:100077. Available from: https://doi.org/10.1016/j.mlblux.2021.100077
3. Terahara F, Nishiura H. Fluoroquinolone consumption and Escherichia coli resistance in Japan: An ecological study. BMC Public Health. 2019;19(1):1–8.
4. Wright L, Heywood N, Cooke FJ, Brown NM. Improving diagnostic stewardship in urinary tract infections: a service evaluation of selective urine culture. J Hosp Infect [Internet]. 2021;117(xxxx):192–3. Available from: https://doi.org/10.1016/j.jhin.2021.07.008
5. Faraday M. The Bakerian Lecture: Experimental Relations of Gold (and Other Metals) to Light. Philos Trans R Soc London [Internet]. 1857;147:145–81. Available from: http://www.jstor.org/stable/108616
6. Erik C. Dreaden, Megan A. Mackey, Xiaohua Huang BK and MAES. Beating cancer in multiple ways using nanogold. R Soc Chem. 2011;40:3391–404.
7. Szunerits S, Spadavecchia J, Boukherroub R. Surface plasmon resonance: Signal amplification using colloidal gold nanoparticles for enhanced sensitivity. Rev Anal Chem. 2014;33(3):153–64.
8. Sánchez-iglesias BA, Pastoriza-santos I, Pérez-juste J, Rodríguez-González B, Abajo FJG De, Liz-marzán LM. Synthesis and Optical Properties of Gold Nanodecahedra with Size Control **. 2006;03(05):2529–34.
9. Ashley MJ, Bourgeois MR, Murthy RR, Laramy CR, Ross MB, Naik RR, et al. Shape and Size Control of Substrate-Grown Gold Nanoparticles for Surface-Enhanced Raman Spectroscopy Detection of Chemical Analytes. J Phys Chem C. 2018;122(4):2307–14.
10. Ying S, Guan Z, Ofoegbu PC, Clubb P, Rico C, He F, et al. Green synthesis of nanoparticles: Current developments and limitations. Environ Technol Innov. 2022;26:102336.
11. OECD. OECD Environmental Outlook to 2050 [Internet]. 2012. 350 p. Available from: https://www.oecd-ilibrary.org/content/publication/9789264122246-en
12. Anastas P, Eghbali N. Green Chemistry: Principles and Practice. Chem Soc Rev [Internet]. 2010;39(1):301–12. Available from: http://dx.doi.org/10.1039/B918763B

13. Tobiszewski M, Mechlinska A, Namie J. Green analytical chemistry—theory and practice. Chem Soc Rev. 2010;39(8):2869–78.
14. Arockiya Aarthi Rajathi F, Parthiban C, Ganesh Kumar V, Anantharaman P. Biosynthesis of antibacterial gold nanoparticles using brown alga, Stoechospermum marginatum (kützing). Spectrochim Acta - Part A Mol Biomol Spectrosc. 2012;99:166–73.
15. Singh P, Kim YJ, Zhang D, Yang DC. Biological Synthesis of Nanoparticles from Plants and Microorganisms. Trends Biotechnol [Internet]. 2016;34(7):588–99. Available from: https://www.sciencedirect.com/science/article/pii/S0167779916000408
16. Narayanan KB, Sakthivel N. Green synthesis of biogenic metal nanoparticles by terrestrial and aquatic phototrophic and heterotrophic eukaryotes and biocompatible agents. Adv Colloid Interface Sci. 2011;169(2):59–79.
17. Mollazadeh H, Hosseinzadeh H. Cinnamon effects on metabolic syndrome: A review based on its mechanisms. Iran J Basic Med Sci. 2016;19(12):1258–70.
18. Nabavi SF, Lorenzo A Di, Izadi M, Sobarzo-sánchez E, Daglia M, Nabavi SM. Antibacterial Effects of Cinnamon: From Farm to Food, Cosmetic and Pharmaceutical Industries. 2015;7729–48.
19. Salim AA, Ghoshal SK, Krishnan G, Bakhtiar H. Tailored fluorescence traits of pulse laser ablated Gold-Cinnamon nanocomposites. Mater Lett [Internet]. 2020;264:127335. Available from: https://doi.org/10.1016/j.matlet.2020.127335
20. Senanayake UM, Lee TH, Wills RBH. Volatile Constituents of Cinnamon (Cinnamomum zeylanicum) Oils. J Agric Food Chem. 1978;26(4):822–4.
21. Rao PV, Gan SH. Cinnamon: A multifaceted medicinal plant. Evidence-based Complement Altern Med. 2014;2014.
22. Vangalapati M, Sree Satya N, Surya Prakash D V., Avanigadda S. A review on pharmacological activities and clinical effects of Cinnamon species. Res J Pharm Biol Chem Sci. 2012;3(1):653–63.
23. Langford JI, Wilson AJC. Scherrer after sixty years: A survey and some new results in the determination of crystallite size. J Appl Crystallogr [Internet]. 1978;11(2):102–13. Available from: https://doi.org/10.1107/S0021889878012844
24. Monshi A, Foroughi MR, Monshi MR. Modified Scherrer Equation to Estimate More Accurately Nano-Crystallite Size Using XRD. 2012;2012(September):154–60.
25. Schneider, C., Rasband, W. & Eliceiri K. NIH Image to ImageJ: 25 years of image analysis. Nat Methods [Internet]. 2012;9:671–675. Available from: https://doi.org/10.1038/nmeth.2089
26. Salim AA, Bidin N, Ghoshal SK, Islam S, Bakhtiar H. Synthesis of truncated tetrahedral cinnamon nanoparticles in citric acid media via PLAL technique. Mater Lett [Internet]. 2018;217:267–70. Available from: https://doi.org/10.1016/j.matlet.2018.01.103
27. Barnard AS, Young NP, Kirkland AI, Van Huis MA, Xu H. Nanogold: A quantitative phase map. ACS Nano. 2009;3(6):1431–6.

28. Huang J, Sun J, Warden AR, Ding X. Colorimetric and photographic detection of bacteria in drinking water by using 4-mercaptophenylboronic acid functionalized AuNPs. Food Control. 2020;108(September 2019):106885.

Figures

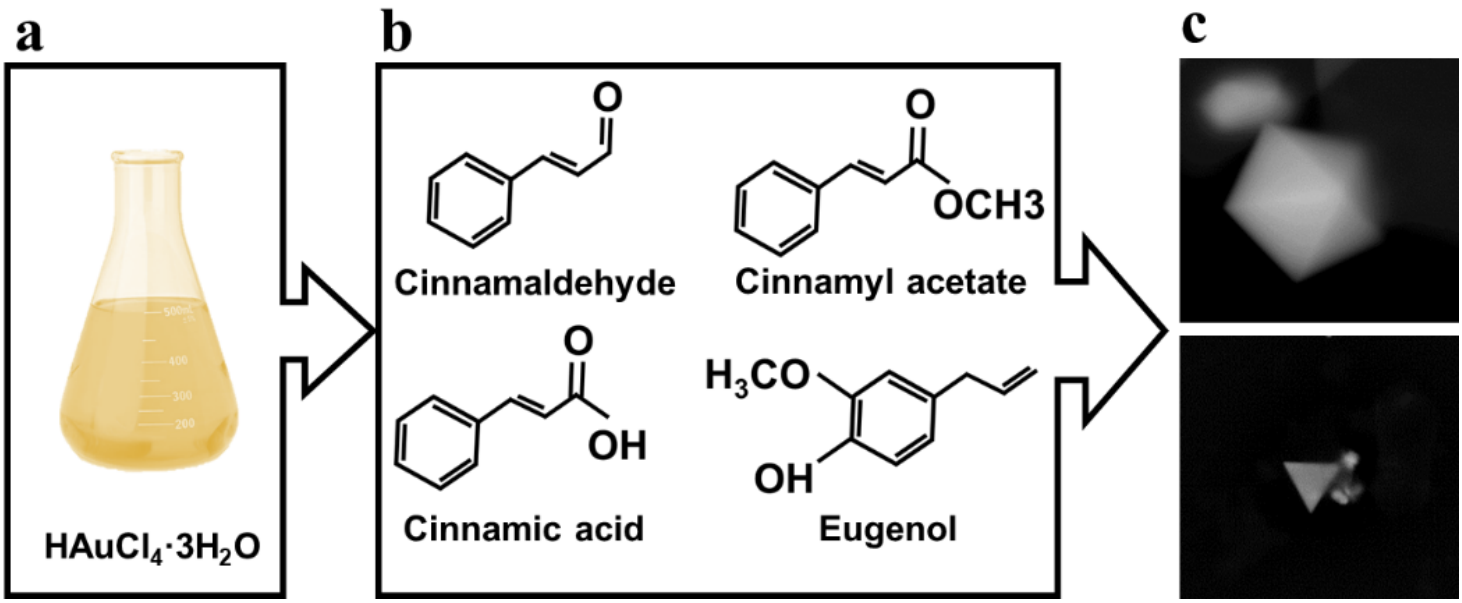


Figure 1

Schematic representation showing the essential components for the process of reduction of Au^{+} into AuNPs; a) salt gold precursor used, b) principal chemical constituents of *Cinnamomum verum* extract [17,21] and c) AuNPs obtained via green chemistry synthesis.

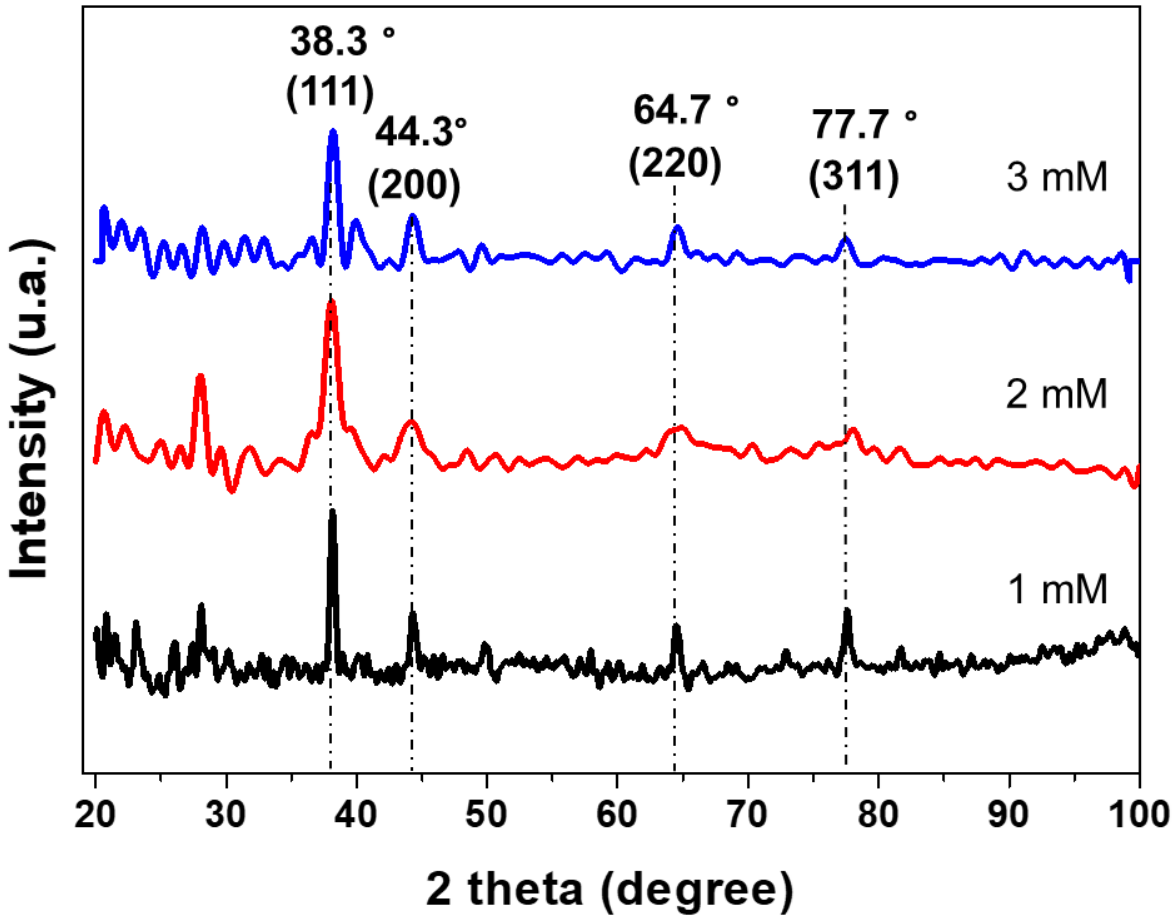
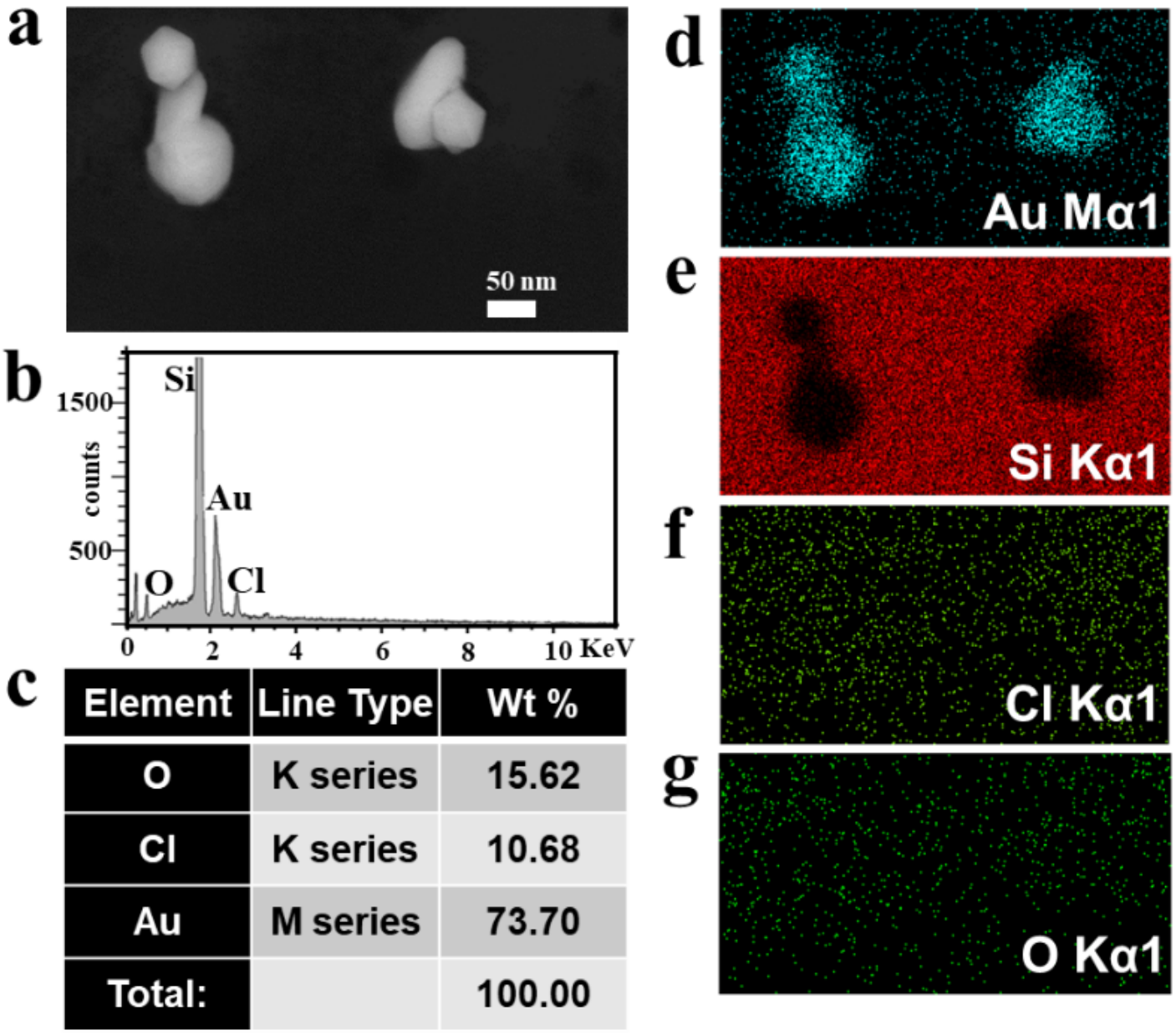


Figure 2

XRD analysis of the AuNPs with three different molar concentrations, obtained after depositing a drop of the AuNPs colloidal on amorphous silicon substrate.



Element	Line Type	Wt %
O	K series	15.62
Cl	K series	10.68
Au	M series	73.70
Total:		100.00

Figure 3

(a) HR-FESEM image of AuNPs supported on silicon, (b) EDS spectra indicating the presence of individual elements, (c) Table indicating the wt % of individual elements, (d-g) gold, silicon, chlorine and oxygen EDS map, respectability.

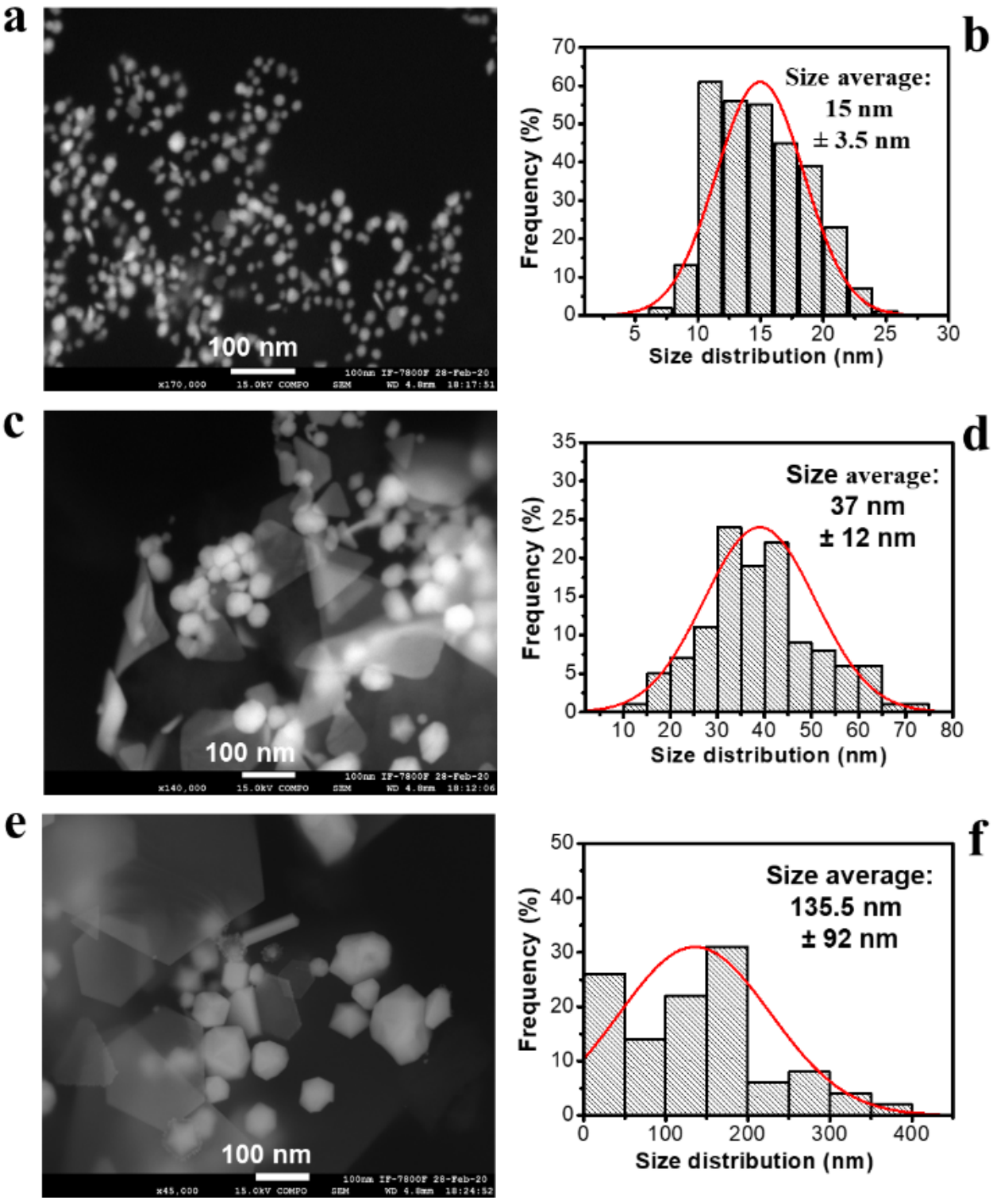


Figure 4

Morphology of AuNPs using *Cinnamomum verum* extract and its representative HR-SEM micrographs. (a-b) AuNPs concentration 1 mM and its size distribution, (c-d) AuNPs concentration 2 mM and its size distribution and (e-f) AuNPs concentration 3 mM and its size distribution.

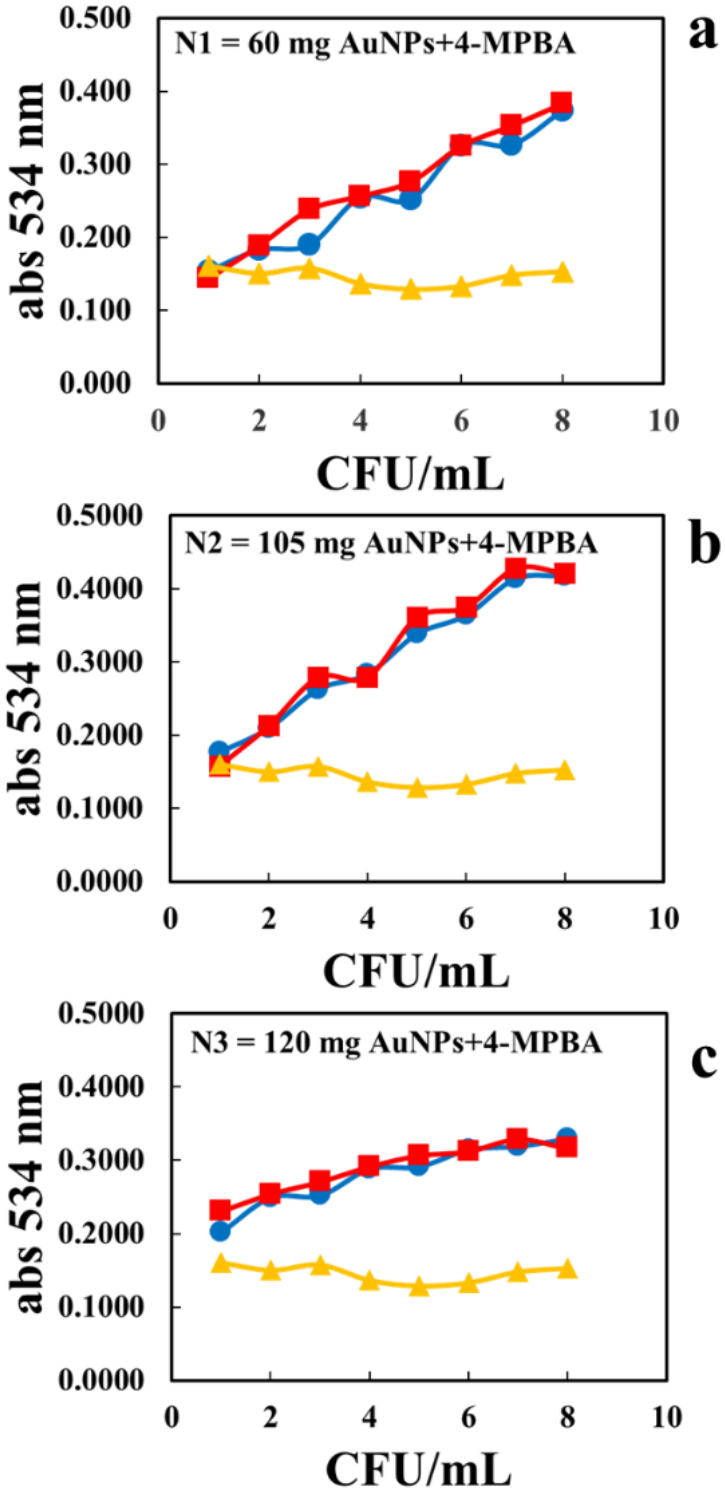


Figure 5

Detection via UV-vis spectroscopy showing the effect of using different concentrations of functionalized AuNPs, the red-line (square symbol) contained urine with different bacteria concentrations, blue-line (circle symbol) corresponds to functionalized AuNPs at their respectively concentration in water with different bacteria concentrations. The yellow-line (triangular symbol) corresponds to water with bacteria

at different concentrations; a) concentration of 60 mg, b) concentration of 105 mg and c) concentration of 120 mg of AuNPs, respectability.

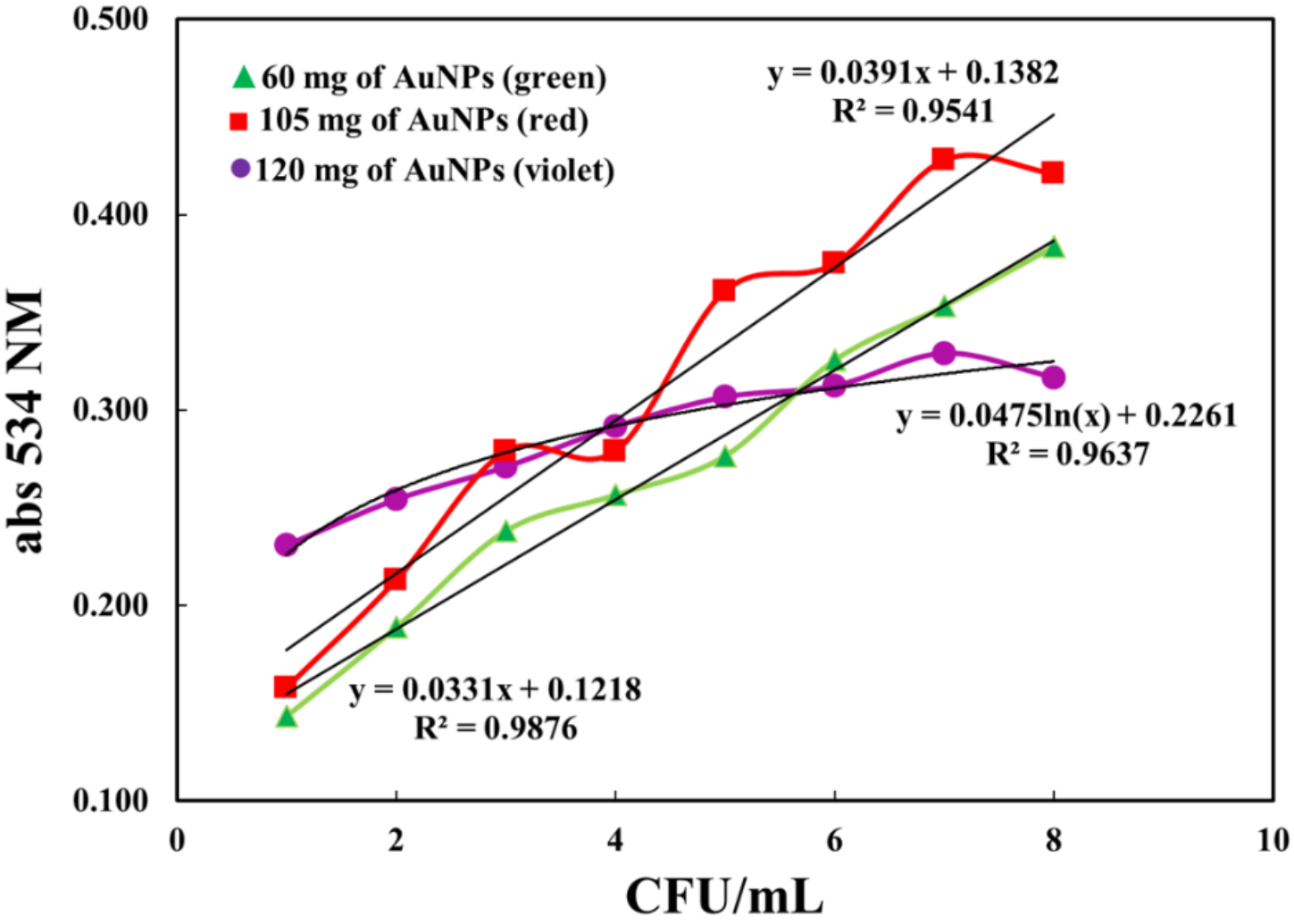


Figure 6

Linear fitting between the absorbance intensity at 534 nm and the bacteria concentration *E. Coli* (10^1–10^8 CFU/mL) in 60, 105 and 120 mg of functionalized AuNPs.